

# Temperature-Controlled Growth of Silicon-Based Nanostructures by Thermal Evaporation of SiO Powders

Z. W. Pan,<sup>†</sup> Z. R. Dai,<sup>†</sup> L. Xu,<sup>‡</sup> S. T. Lee,<sup>‡,\*</sup> and Z. L. Wang<sup>\*,†,§</sup>

School of Materials Science and Engineering, Georgia Institute of Technology, Atlanta, Georgia 30332-0245, Center of Super-Diamond and Advanced Film, Department of Physics and Materials Science, City University of Hong Kong, Kowloon, Hong Kong

Received: November 20, 2000; In Final Form: January 17, 2001

Silicon-based nanostructures with different morphologies, sizes, compositions, and microstructures were grown on Si wafers by thermal evaporation of SiO powders at 1350 °C for 5 h under 300 Torr of a flowing gas mixture of 5% H<sub>2</sub>-Ar at a flow rate of 50 standard cubic centimeters per minute (sccm). The SiO powders and Si wafers were placed inside an alumina tube, which was heated by a tube furnace. The local temperature inside the tube was carefully calibrated by a thermal couple. After evaporation, Si-containing products with different colors and appearances were formed on the surfaces of the Si wafers over a wide temperature range of 890–1320 °C and a long distance of ~85 mm. Basing on the colors and appearances of the products, five distinct zones, which corresponding to different temperature ranges, were clearly identified from the highest temperature of 1320 °C to the lowest temperature of 890 °C. They are zone I (1250–1320 °C), zone II (1230–1250 °C), zone III (1180–1230 °C), zone IV (930–1180 °C), and zone V (890–930 °C). The deposited products were systematically studied by scanning electron microscopy, transmission electron microscopy, and X-ray diffraction. The results show that, besides Si nanowires, many other kinds of Si-based nanostructures such as octopuslike, pinlike, tadpolelike, and chainlike structures were also formed. The temperature distribution inside the alumina tube was found to play a dominant role on the formation of these structures. It is demonstrated that a control over the growth temperature can precisely control the morphologies and intrinsic structures of the silicon-based nanomaterials. This is an important step toward design and control of nanostructures. The growth mechanisms of these products were briefly discussed.

## 1. Introduction

Silicon-based nanoscale materials have attracted much attention in recent years for their valuable semiconducting, mechanical, and optical properties, as well as their potential applications in mesoscopic research and nanodevices. They are, for example, considered as candidates for one-dimensional quantum transistors, composites, and light-emitting diodes.<sup>1</sup> Consequently, a great deal of effort has been made in fabricating Si-based nanostructures, especially Si nanowires. Several techniques have been developed to produce Si nanowires, including lithography and etching,<sup>2–4</sup> scanning tunneling microscopy,<sup>5,6</sup> vapor–liquid–solid (VLS) growth,<sup>7–10</sup> laser ablation of metal-containing Si target<sup>11–14</sup> or metal-free Si/SiO<sub>2</sub> target,<sup>11,15</sup> and thermal evaporation of Si–SiO<sub>2</sub> mixture<sup>11,16,17</sup> or SiO powders.<sup>11,18</sup>

Among these techniques, the thermal evaporation technique developed by Lee et al.<sup>11</sup> is of particular interest and has attracted much attention in recent years due to its low cost and ease of manufacture. By using SiO powders as the source material, this technique can be used to easily produce a large quantity of high-purity (no metal contamination), ultralong (in millimeters), and uniform-sized (a few nanometers to tens of nanometers in diameter) Si nanowires. The quality of the Si

nanowires produced by this technique is comparable to those produced by traditional VLS<sup>7–10</sup> and laser ablation.<sup>11–15</sup> In thermal evaporation, oxides were found to play a dominant role in the nucleation and growth of Si nanowires. The growth mechanism of Si nanowires from thermal evaporation of SiO powders, however, is not fully understood. Thus, more detailed and systematic experimental investigations are required.

In this paper, we systematically investigate nanomaterials produced from thermal evaporation of SiO powders as a function of the local temperature. Our results show that, besides Si nanowires, many other kinds of Si-based nanostructures such as octopuslike, pinlike, tadpolelike, and chainlike structures were also formed at different temperature zones. Our experiments show that control of the temperature can also control the morphology, size, crystallization, and composition of the Si-based nanostructures.

## 2. Experimental Method

The apparatus used for thermal evaporation of SiO powders is schematically shown in Figure 1. An alumina tube was mounted inside a horizontal tube furnace. A 3–5 g sample of 99.9% pure SiO powder (from Aldrich) was placed in an alumina crucible and located at the center of the alumina tube. Several striplike Si wafers (60 mm in length and 10 mm in width) were placed one by one on a long alumina plate (15 cm in length and 20 mm in width) to act as the deposition substrates for the grown materials. SiO is dark brown and SiO<sub>2</sub> is transparent white. The position of the alumina plate inside the

\* Corresponding authors. E-mail: zhong.wang@mse.gatech.edu (ZLW), and APANNALE@cityu.edu.hk (STL).

<sup>†</sup> Georgia Institute of Technology.

<sup>‡</sup> City University of Hong Kong.

<sup>§</sup> School of Materials Science and Engineering and School of Chemistry and Biochemistry, Georgia Institute of Technology.

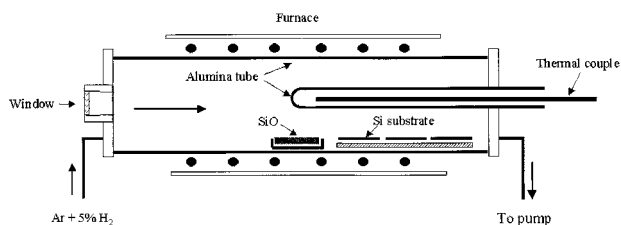


**Figure 1.** Schematic diagram of the experimental setup.

alumina tube was exactly measured to correlate the formation of products with local temperature. Before evaporation, the alumina tube was evacuated to  $\sim 2 \times 10^{-3}$  Torr by a mechanical rotary pump. Finally, SiO<sub>2</sub> powders were heated at 1350 °C for 5 h under a pressure of 300 Torr; 5% H<sub>2</sub>-Ar gas mixture was kept flowing through the tube at a flow rate of 50 sccm. During evaporation, the growth status inside the alumina tube could be viewed in situ through a quartz window located at the gas inlet end of the alumina tube.

To measure the temperature distribution along the downstream direction inside the alumina tube, a thinner alumina tube was inserted into the larger one along its axis. One end of the thinner tube was closed and located at the center of the furnace, while the other end was open and extended outside the furnace. A thermocouple, which was inserted inside the thinner tube and could be moved freely along the tube axis, was used to measure the temperature inside the larger tube. During evaporation, the temperature at any point between the tube center and the tube's downstream end could be measured in situ by using this temperature measuring device. Thus, the relationship between local temperature and products could be readily obtained.

After evaporation, the alumina plate, together with the silicon wafers on it, were carefully removed from the alumina tube without disturbing the sequence of the deposited products. This is important for correlating the structures of the local deposited materials with the temperature. The morphologies of the as-deposited products were examined by scanning electron microscopy (SEM) (Philips XL 30 FEG); the microstructures were investigated by transmission electron microscopy (TEM) (Hitachi HF2000 FE-TEM at 200 kV) and high-resolution TEM (HRTEM) (JEOL 4000EX at 400 kV); the crystalline state was analyzed by X-ray diffraction (XRD) (Philips, PW1800 using Cu K $\alpha$  radiation); the chemical composition was determined by energy-dispersive X-ray spectroscopy (EDS) attached to the SEM and Hitachi HF2000 FE-TEM.

### 3. Experimental Results

Products formed at different temperature zones are distinctly different in color. Simply by observing the products with the naked eye, it can be found that, after 5 h of growth at 1350 °C under 300 Torr with a carrier gas flow rate of 50 sccm, products with different colors and appearances were formed over a wide temperature range between 890 and 1320 °C within a distance of  $\sim 85$  mm inside the tube. From the highest temperature of 1320 °C to the lowest temperature of 890 °C, the color of the products changed from dark gray to bright yellow, yellow mixed with pink, light yellow, and finally brown. The corresponding appearance of the deposited products changed from round-tip short rods to circular hard shell, fine powders, spongelike wires, and finally long and straight microscale wires, respectively. On the basis of the colors and appearances described above, five distinctive temperature zones were identified: zone I (1250–1320 °C), zone II (1230–1250 °C), zone III (1180–1230 °C), zone IV (930–1180 °C), and zone V (890–930 °C). Figure 2

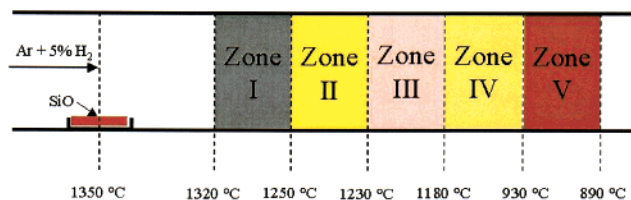


**Figure 2.** Schematic diagram of the five distinctive growth zones inside the alumina tube. The colors and temperature ranges of these zones are also shown.

schematically depicted the position and the corresponding temperature of the five zones inside the alumina tube.

#### 3.1. Zone I (1250–1320 °C).

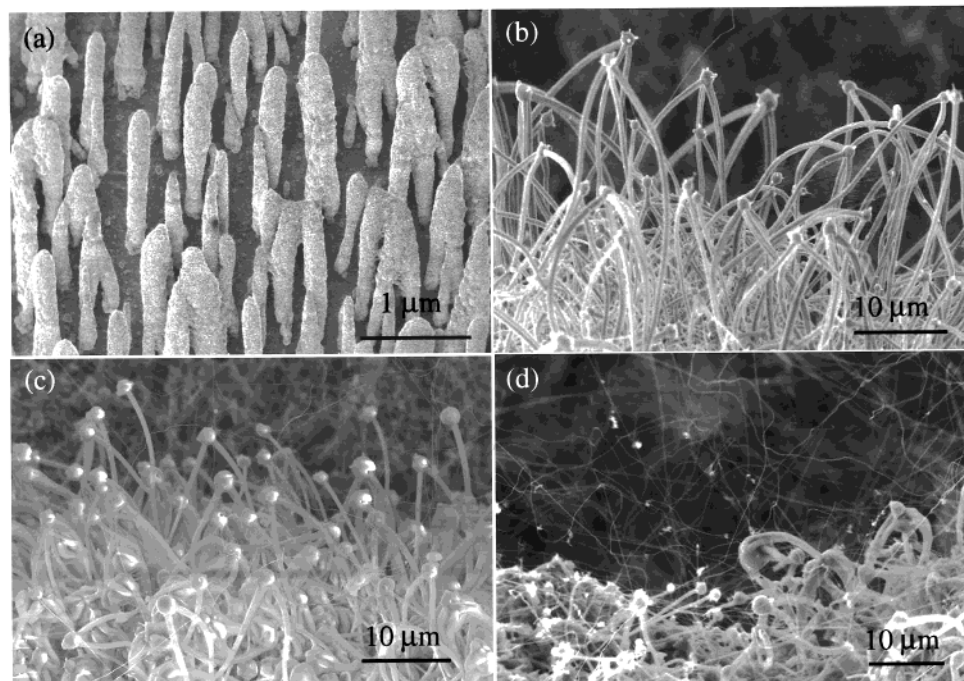
The products formed in zone I were dark gray. The length of this zone is about 35 mm. Low-magnification SEM image reveals that a large quantity of round-tip rods with 50–200  $\mu\text{m}$  diameters and of 0.5–2 mm length were formed in zone I (Figure 3a). These rods decline to the silicon substrate along the flowing direction of the carrier gas at almost the same angle, forming “aligned” structures. High-magnification SEM studies show that the rods were mainly composed of three kinds of structures: octopuslike structure (Figure 3b), pinlike structure (Figure 3c), and nanowires (Figure 3d).

Figure 3b shows a SEM image of the octopuslike structures. This kind of structure has been observed in samples prepared by heating SiO<sub>2</sub> on a Ta heater at 1600 °C.<sup>19</sup> Usually, the octopuslike structure has two to five arms sprout from its spherical tip. The typical diameters of the tips are in the range of 1–2  $\mu\text{m}$ . The arm surfaces are smooth, and their diameters gradually decrease as the distance from the tips increase. TEM observations (Figure 4a) and EDS analysis show that the tip of the octopuslike structure is a crystalline Si ball covered with a thin amorphous silicon oxide layer, while the arm is a crystal Si wire sheathed with a thick amorphous outer layer of silicon oxide. The composition of silicon oxide has been determined as SiO<sub>2-x</sub>, where  $x = 0-0.5$ . HRTEM investigations (Figure 4b) reveal that the Si wire is well-crystallized and has a growth direction close to (112), which is different from the (111) growth direction of the Si whiskers prepared by the metal-catalyzed VLS reaction.<sup>7-10</sup>

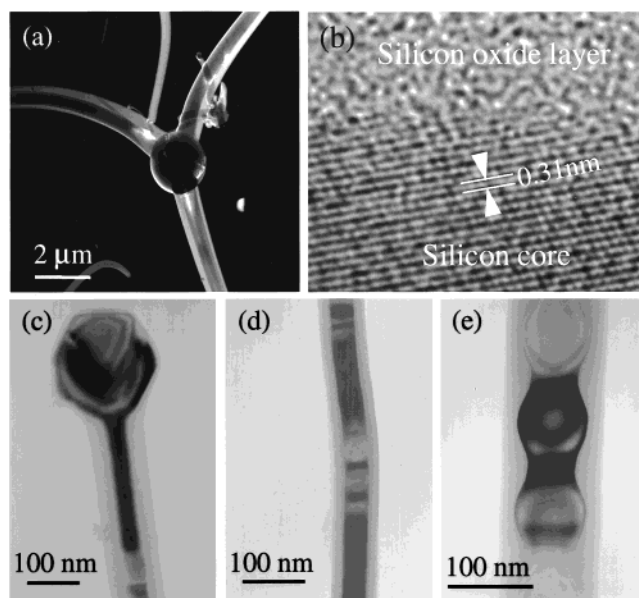
From Figure 3b it can also be clearly seen that, in contrast to the long arms that sprout from the lower side of the spherical tip, a few (usually one to four) very short rods extrude from the upper side of the tip. It seems from the morphology that, if the growth time were long enough, these short rods would grow into long arms such as those located at the lower side of the tip. Therefore, we suggest that these short rods might act as the nucleation sites of the arms from which the octopuslike structure was formed.

Figure 3c shows a SEM image of the pinlike structures. Each “pin” consists of a wire and a ball at its tip. The diameters of the wires and tips are in the ranges of 0.3–0.8 and 0.5–1.5  $\mu\text{m}$ , respectively, which are smaller than those of the octopuslike structures. The length of the wires is in the range of 10–50  $\mu\text{m}$ . TEM studies (Figure 4c) show that the pinlike structure has the same microstructure as the octopuslike structure; namely, the tip is a Si ball covered with a thin silicon oxide layer and the wire has a Si core and a thick silicon oxide outer sheath.

In zone I, there also exist many nanowires on the surface of the round-tip rods, as shown in Figure 3d. These nanowires have a quite uniform diameter of  $\sim 100$  nm and a very long length of up to several millimeters. TEM studies indicate that the wires have a core-shell structure (Figure 4d); namely, each wire consists of a crystalline Si core and an amorphous outer layer



**Figure 3.** SEM images of the nanomaterials formed in zone I. A large quantity of dark gray aligned round-tip rods were formed in this zone (a). These rods were mainly composed of octopuslike (b), pinlike (c), and wirelike (d) structures.



**Figure 4.** TEM and HRTEM images of the products formed in zone I. (a) Dark field TEM image of an octopuslike structure. (b) HRTEM image of the arm of the octopuslike structure shown in (a). (c) TEM image of the pinlike structure. TEM images of the Si nanowire with uniform Si core (d) and bulblike Si core (e).

of silicon oxide. Occasionally, the Si core exhibits bulblike morphology, but the outer oxide sheath keeps a uniform diameter (Figure 4e). HRTEM investigations show that the microstructure of the nanowire is similar to that of the octopuslike structure shown in Figure 4b. The growth direction of the nanowires is generally along  $\langle 112 \rangle$ .

### 3.2. Zone II (1230–1250 °C).

A bright yellow circular hard shell with outer diameter equal to that of the alumina tube was formed in the region with temperatures of 1230–1250 °C. By in situ observing the growth status through the quartz window, we found that the shell was initially formed from the inner wall of the alumina tube and

then grew radially toward the tube center to form a circular shell. If the growth time is long enough, the circular shell will finally grow into a disklike shell. As a result, the disklike shell will block up the alumina tube and thus stop the gas flowing through the tube. The thickness of the shell at the inner wall of the alumina tube is about 3 mm and then decreases gradually as the distance from the wall increases. The shell is brittle and can be easily broken into small pieces.

Low-magnification SEM examination on the surface of the hard shell reveals the presence of numerous fine pinlike nanowires (Figure 5a). The diameters of the tips and wires are in the ranges of 50–200 and 30–100 nm, respectively, which are much smaller than those of the pinlike structures formed in zone I. The length of the wires is in the range of 2–10 μm. It should be noted that no apparent octopuslike structures are present on the shell surface.

Figure 6a shows the low-magnification TEM image of the pinlike nanowires. Clearly, each wire has a round tip and a sharp tail. High-magnification TEM observation reveals that the tips are not strictly round in shape; instead, most of the tips exhibit a polyhedral structure and a typically hexagonal cross section is often observed (Figure 6b). Both TEM examination and EDS analysis reveal that the tip of the pinlike nanowire is composed of a crystalline Si ball and a very thin amorphous silicon oxide layer, while the wire is either amorphous silicon oxide (for the wires with diameter < 50 nm) (Figure 6b) or a crystalline Si core sheathed with silicon oxide layer (for the wires with diameter > 50 nm) (Figure 6c). It should be noted that, for the core–shell structure as that shown in Figure 6c, the length of the Si core is only one-third to one-half of the entire length of the wire, and the rest of the wire is pure amorphous silicon oxide.

We also investigated the cross section of the hard shell by SEM. Surprisingly, the structure of the cross section of the shell was quite different from the surface structure. Two typical images taken from the cross section of the hard shell are shown in Figure 5b,c, where two major forms can be identified. One form consists of chains of nanoparticles (Figure 5b), while the

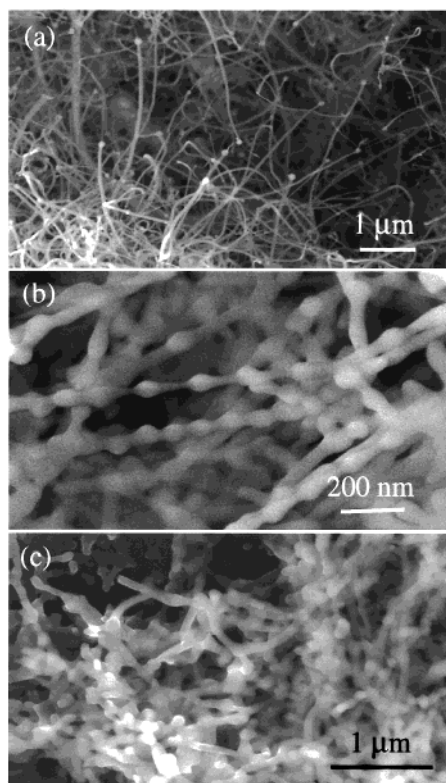


**Figure 5.** SEM images of the products formed in zone II. A yellow circular hard shell was formed in this zone inside the growth tube. The surface of the hard shell was composed of numerous pinlike nanowires (a), while the cross section of the shell was composed of sintered particle chains (b) and short bars (c).

other form is a short bar with length less than  $1 \mu\text{m}$  (Figure 5c). The morphologies shown in Figure 5b,c might have resulted from the sintering of the pinlike nanowires that initially formed and are present on the surface of the shell, due to long time at high temperature.

### 3.3. Zone III (1180–1230 °C).

Products with a color of yellow mixed with pink were formed in zone III. The length of this zone is about 5–10 mm. Usually, a few pink stripes and a few yellow stripes, perpendicular to the alumina tube axis, coexist one after the other. Under the naked eye and optical microscopy, these pink and yellow products are powderlike, but under SEM, the yellow product mainly consists of fine pinlike structures (Figure 7a), while the pink product mainly consists of tadpolelike structures (Figure 7b).

TEM investigations reveal that, as the case shown in Figure 6, the pinlike nanowires formed in zone III in yellow also consist of a crystalline Si tip and a wire composed of either amorphous silicon oxide (for the thin wires) or a Si core sheathed with amorphous silicon oxide layer (for the thick wires).

Figure 8a shows a low-magnification TEM image of the tadpolelike structures from the pink stripes. It is clearly that the tadpolelike structure is actually a chain of pins, in which several pins connect together with the head of one connecting to the tail of another. In Figure 8b, 20 pins connect one by one to form a close circle. Higher magnification TEM examinations show that the particles in the tadpolelike structures are crystalline Si, while the bars between the particles are either amorphous silicon oxide (Figure 8c) or a core-shell structure (Figure 8d).

### 3.4. Zone IV (930–1180 °C).

Large quantities of Si nanowires were formed in zone IV. The nanowire products covered approximately 30 mm in length

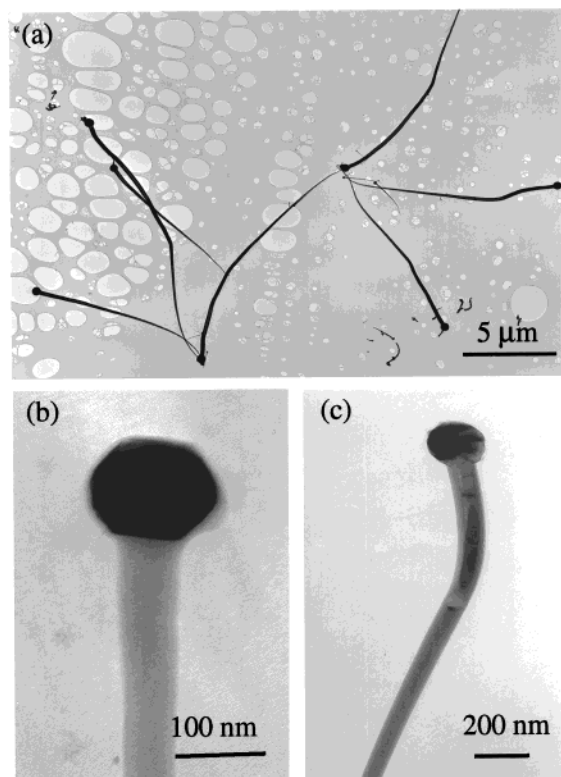


**Figure 6.** TEM images of the pinlike nanowires formed in zone II. The pinlike wires have a round tip and a sharp tail (a). The tip is crystalline Si, while the wire is either amorphous (b) (for thin wires) or a Si core sheathed with silicon oxide layer (c) (for thick wires).

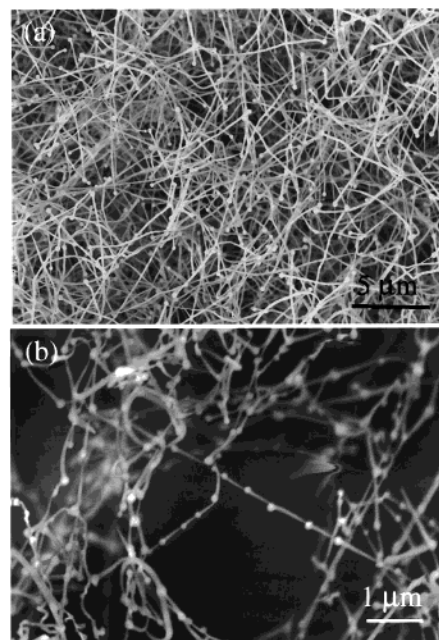


**Figure 7.** SEM images of the products formed in zone III. The color of the products formed in this zone is yellow mixed with pink. The yellow product is composed of very fine pinlike nanowires (a), while the pink product is composed of tadpolelike nanostructures (b).

of the Si substrate. The Si nanowires formed in this zone have been intensively studied previously by Lee et al.<sup>11,14–16,18</sup> Under optical microscopy, zone IV can be clearly divided into two regions with almost equal length by the color and morphology of the wires. In the front region (the corresponding temperature range is 1050–1180 °C), light yellow nanowires closely attach

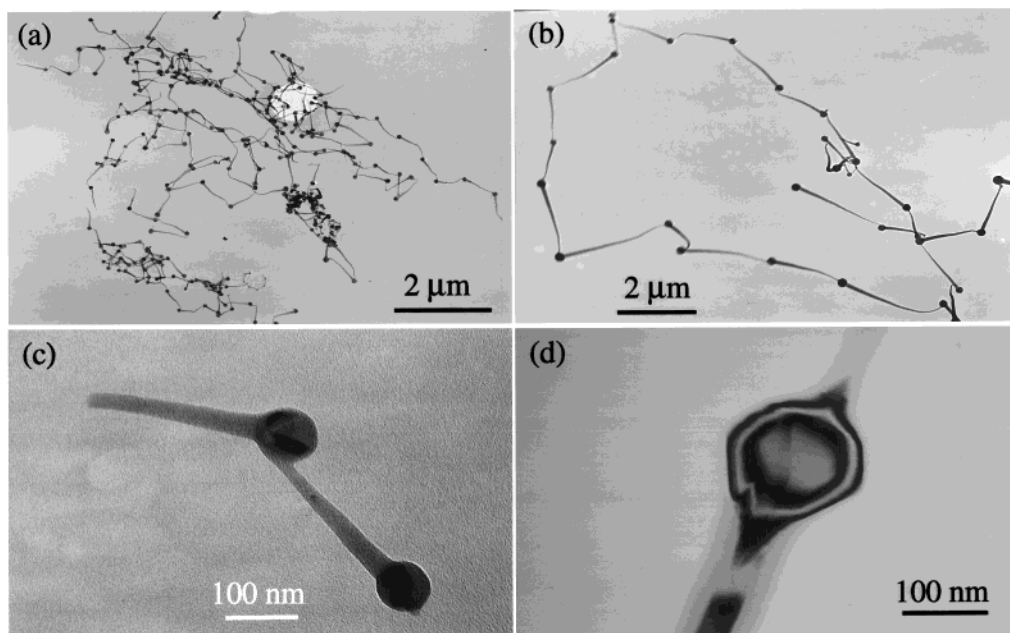


**Figure 8.** TEM images of the tadpolelike nanostructures (a and b). The particles in the tadpolelike structures are crystalline Si, while the bars between the particles are either amorphous silicon oxide (c) or a Si core sheathed with amorphous silicon oxide layer (d).

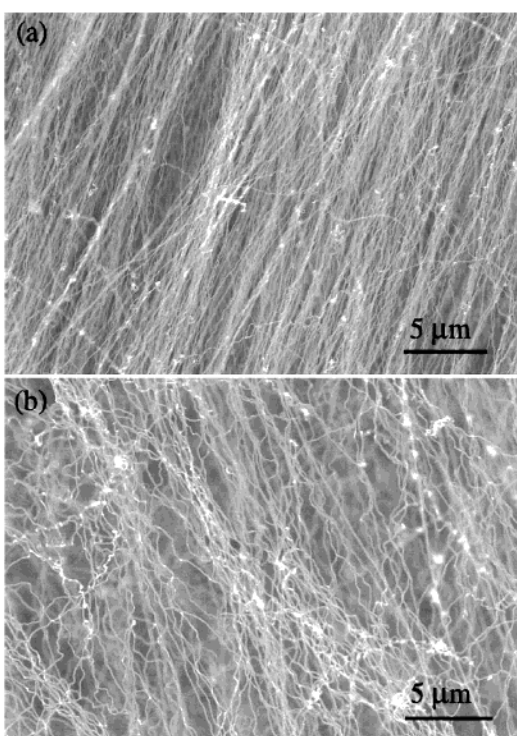


**Figure 9.** SEM images of the products formed in zone IV. The products formed in this zone are light yellow (a) and white yellow (b) Si nanowires, which grow along the flowing direction of the carrier gas and form quasi-aligned structures.

to the surface of Si substrate to form a nanowire film. In SEM images, these nanowires appear to have an aligned structure (Figure 9a), in which the nanowires grow along the same direction that is parallel to the direction of the flowing carrier gas. This phenomenon was recently reported by Shi et al.<sup>20</sup> The thickness of the aligned Si nanowire film is about 10–20  $\mu\text{m}$ . In the back region (the corresponding temperature range is 930–1050  $^{\circ}\text{C}$ ), a large amount of white yellow Si nanowires tangle together to form a thick (1–3 mm in thickness) spongelike domain. SEM observation reveals that although the wires are

curled and tangled, they still exhibit more or less aligned features (Figure 9b).

TEM and HRTEM studies of the morphologies and structures show no apparent difference between the Si nanowires formed in the front region and those formed in the back region. A typical morphology of the Si nanowires is shown in Figure 10a, where two kinds of wires can be identified. One kind is Si nanowires with uniform diameters (20–30 nm) and a smooth surface. HRTEM examinations show that each wire consists of a crystalline Si core and an outer layer of silicon oxide (Figure 10b), which is similar in microstructures to the Si nanowires formed in zone I. However, by comparing Figure 10b with Figure 4d,e, it can be found that the Si cores of nanowires formed in zone IV are usually discontinuous, indicating that the nanowires formed in zone IV have a poorer crystallinity than the wires formed in zone I. A high density of defects, such as stacking faults and microtwins, were usually observed in the crystalline Si core of the wire.

The other kind of wires consists of chains of Si nanoparticles. HRTEM investigations reveal that the Si nanoparticles in the chain are Si crystals with different orientations, while the short bars between the Si nanoparticles are amorphous silicon oxide (Figure 10c).

### 3.5. Zone V (890–930 $^{\circ}\text{C}$ ).

The color of the products formed in zone V is similar to that of the source material SiO. From the higher temperature of 930  $^{\circ}\text{C}$  to the lower temperature of 890  $^{\circ}\text{C}$ , wires with color from light brown to brown and finally to dark brown were formed. The length of zone V is about 10 mm. In fact, except for color, no visible difference could be distinguished by the naked eye between the adjacent light brown wires in zone V and the white yellow wires in zone IV. However, under SEM, the diameters of the light brown wires are apparently larger than the white yellow wires. Parts a, b, and c of Figure 11 show the images taken from samples with colors of light brown, brown, and dark brown, respectively. Two main features can be obtained from these images: (i) the wires formed in zone V are highly aligned with the growth direction parallel to the flowing direction of the carrier gas. The diameters of the light brown, brown, and dark brown wires are in the ranges of 50–200 nm, 0.5–1  $\mu\text{m}$ ,

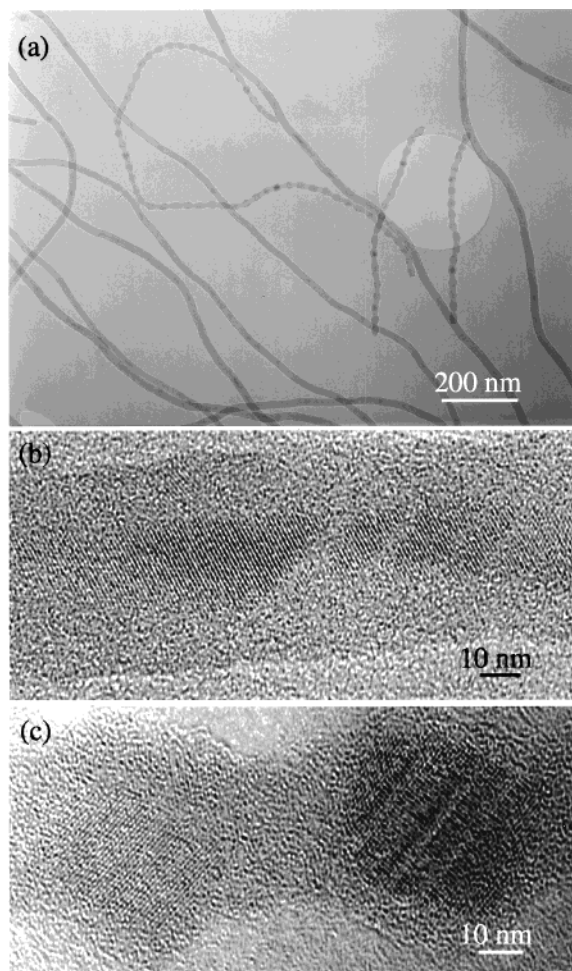


**Figure 10.** (a) TEM images of the Si nanowires formed in zone IV, showing two major morphologies. One is Si core sheathed with an amorphous silicon oxide outer layer (b); the other is chains of Si particles with different orientation (c).

and 1–5  $\mu\text{m}$ , respectively. All of the wires are straight and long with lengths up to 3–5 mm. (ii) The surface of the wires is severely roughened. No crystal growth characteristics can be found from the morphologies of the wires. EDS analysis reveals that the wires are composed of SiO.

XRD results taken from the above five zones are summarized in Figure 12. For the sake of comparison, the XRD spectrum of SiO powders was also shown in Figure 12. It can be seen that the samples formed in zones I, II, and III have almost the same XRD spectra, in which several sharp peaks of cubic  $\beta$ -Si and a broad peak of silicon oxide coexist. In contrast, the Si nanowires formed in zone IV exhibit weaker Si peaks and a stronger silicon oxide peak, which indicates that the Si nanowires formed in zone IV have a lower crystallinity than the products formed in zones I–III and/or the volume fraction of Si structure is relatively lower. This is consistent with the TEM results shown above. The XRD spectrum taken from the wires formed in zone V reveals that these wires are almost amorphous. It is apparent in Figure 12 that the XRD spectrum of the wires formed in zone V is similar to that of the SiO powders, which indicates that the wires formed in zone V are mainly composed of SiO. This finding agrees well with the EDS results.

#### 4. Discussion

The results described in Section 3 show that, by thermal evaporation of SiO powders at 1350  $^{\circ}\text{C}$  for 5 h under 300 Torr

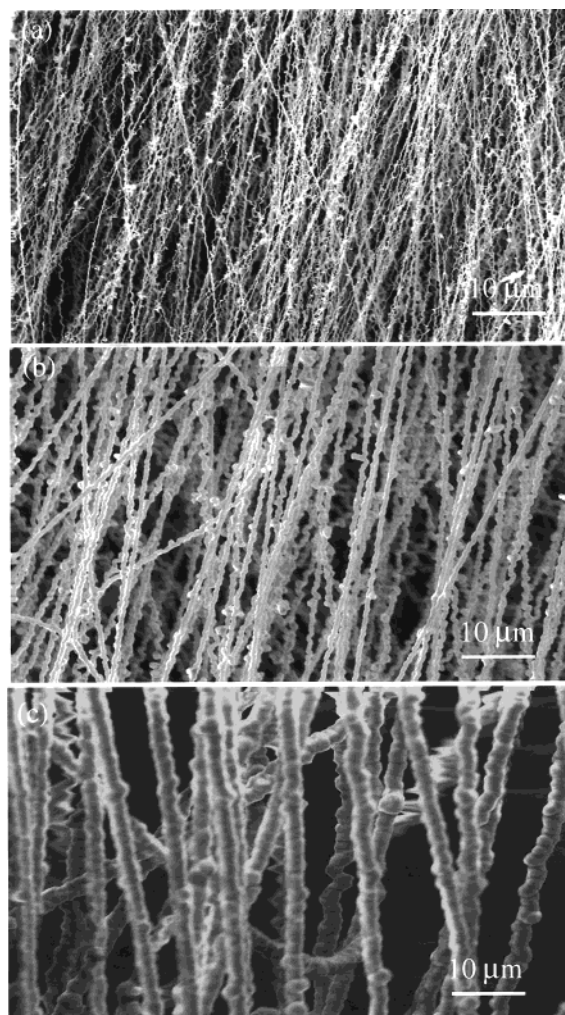


**Figure 11.** SEM images of the products formed in zone V. The products formed in this zone are light brown (a), brown (b), and dark brown (c) amorphous SiO wires (from high temperature to low temperature).

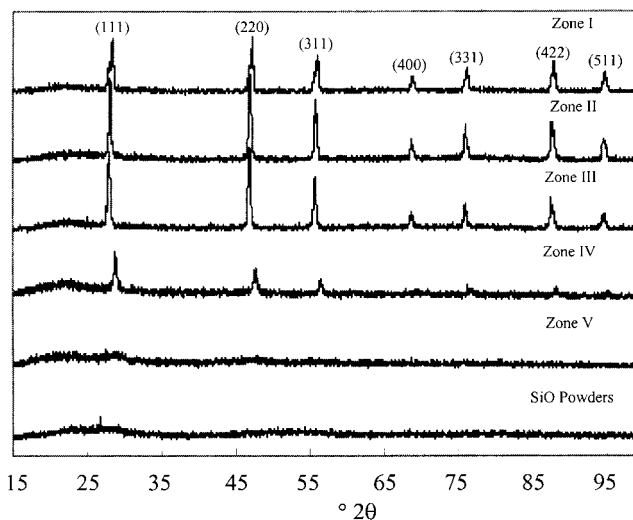


**Figure 12.** XRD spectra of the products formed in zones I–V, as well as the source material SiO powders.

of a 5%  $\text{H}_2$ -Ar gas mixture at a flow rate of 50 sccm, Si-containing products with different morphologies, sizes, compositions, and microstructures were formed over a wide temperature range between 890 and 1320  $^{\circ}\text{C}$  and a long distance of about 85 mm. Our extensive experiments at varied furnace

temperatures (1200–1400 °C) show that the products were strongly related to the temperature distribution inside the alumina tube. Within a specific temperature range, products with a specific color, morphology, and microstructure were formed. The color character may be accounted for by two factors: one is the nonuniform distribution of SiO and SiO<sub>2</sub> on the surface, where the former is dark brown and the latter is white; and the other is the different morphologies of the products. Both SiO and SiO<sub>2</sub> are amorphous, and they are very difficult to distinguish by TEM. Chemical microanalysis may help to identify the phases, but it becomes inconclusive if the phases are in nanoscale. Therefore, we believe that the temperature distribution inside the alumina tube has a dominant influence on the formation of different products. Now, the question is, how were these different products formed?

From the information provided by images shown in Figures 3–8, it is clear that the Si-containing octopuslike, pinlike, and tadpolelike structures formed in zones I–III have a common feature: crystalline Si balls are consistently present at the wire's tips. This feature is consistent with the essential feature of the VLS growth, in which a metal catalyst particle is always present at one end of the nanowire (or whisker) to act as the energetically favored site for absorption of gas-phase reactant.<sup>7–10</sup> Although in our case the tips are Si while in traditional VLS they are metals (Au, Fe, or Co), we believe that the function of the Si tips is, to some extent, analogous to that of the metal catalyst. In fact, the catalytic function of the Si tip for wire growth has been shown clearly in Figure 3b, in which several nucleation sites of the wires are extruded from the Si tip.

Since the only source material used in the present study is SiO, we assume that the nucleation of the Si particle occurs on the Si substrate by decomposition of SiO described by  $2\text{SiO} = \text{Si} + \text{SiO}_2$ . After the Si nucleus is formed, it will grow into a larger particle by continuously adsorbing SiO from the vapor phase. To effectively adsorb SiO from the vapor phase, the Si tips should be in or near their molten states (note the melting point of particles is lower than that of bulk). Since the SiO vapor is continuously supplied during the experiment, the molten Si tips will continuously adsorb SiO; as a result, the Si tips will become larger and larger. However, the size of the final Si tip will be limited by the growth temperature; that is, at different temperature zones, the critical value of the molten Si tip is likely to be different. This is evident by comparing the sizes of the tips formed in zones I–III (see Figures 3–8). With consideration of the phase separation of Si and SiO<sub>2</sub>, it is likely that the newly formed molecular silica (on the Si surface) tends to diffuse toward the areas that already have accumulated silica species. SiO<sub>2</sub> is easily deposited and extruded from the Si tip to form either an amorphous silicon oxide sheath (for thick wire) or an amorphous silicon oxide wire (for thin wire). The formed solid SiO<sub>2</sub> component can retard the lateral growth of the nanowires to ensure that the wires grow along one direction to form wirelike nanostructures.

As for the nanowires formed in zone IV, their nucleation and growth process has been investigated in detail in ref 11 by Lee et al. Although these Si nanowires do not apparently have Si tips, their growth can also be attributed to the VLS growth mechanism. It is of course a non-metal-catalyzed VLS growth mechanism.

For the wires formed in zone V, both EDS and XRD results show that these wires are composed of SiO. These results indicate that no decomposition occurs for SiO vapor at temperature below 930 °C. Such a case also occurs in the preparation of Si–O powders from a mixture of SiO<sub>2</sub> and Si.

Hass and Sulzberg<sup>21</sup> found that the decomposition of SiO vapor into Si and SiO<sub>2</sub> should occur above a certain temperature. If the temperature was below this critical temperature (their temperature was 800 °C, 130 °C lower than 930 °C in our case), the SiO vapor directly condensed to form homogeneous amorphous SiO solid. Basing on the results obtained by Hass and Sulzberg and our results described in section 3, it can be concluded that the SiO<sub>2</sub> wires in zone V are formed by directly depositing SiO<sub>2</sub> vapor along one dimension, which is actually a vapor–solid (VS) growth process.

An interesting phenomenon in our experiments is the presence of the aligned structures, e.g., the aligned short rods in zone I, the aligned Si nanowires in zone IV, and the aligned SiO wires in zone V. The growth directions of these aligned structures are all parallel to the flowing direction of the carrier gas, indicating that the formation of these aligned structures may be related to the flow of the carrier gas. This point is confirmed by our extended experiments, which show that, if the gas flow rate is higher, the aligned feature is much more apparent.

The growth of Si-based nanostructures by evaporation of SiO is a rather complicated process. Some experimental phenomena are still not fully understood, including the following: (i) In zone I, why do the octopuslike and pinlike structure accumulate together to form the round-tip short rods? (ii) In zone II, why do the pinlike nanowires sinter together to form a circular hard shell in the growth tube? (iii) In zone III, why do the pinlike wires form a nearly perfect tadpolelike structure by accurately connecting the head of one to the tail of another? (iv) In zone IV, why are the Si nanoparticles present in the form of long chains? (v) In zone V, why can SiO be redeposited along one dimension to form amorphous SiO wires? It is certain that much experimental and theoretical work is needed to answer these questions.

## 5. Conclusion

Silicon-based nanostructures with different colors, morphologies, and microstructures were formed over a wide temperature range from 890 to 1320 °C by thermal evaporation of SiO powders at 1350 °C for 5 h under 300 Torr of a flowing gas mixture of 5% H<sub>2</sub>–Ar at a flow rate of 50 sccm. Silicon-based nanostructures with morphologies such as octopuslike, pinlike, tadpolelike, chainlike, and wirelike were formed in different temperature ranges. Our experimental data show that the temperature distribution inside the alumina tube plays a dominant role in the formation of these structures. It is demonstrated that control over the growth temperature can precisely control the morphology and intrinsic structure of the silicon-based nanomaterials. This is an important step toward design and control of nanostructures. The Si-based nanostructures could offer great opportunities for fundamental and applied research.

**Acknowledgment.** Thanks to the financial support from US NSF Grant DMR-9733160 and the Georgia Tech Electron Microscopy Center for providing the research facility. ZWP was partially supported by the Research Grants Council of Hong Kong (Project No. 9040459).

## References and Notes

- (1) Alivisatos, A. P. *Science* **1996**, *271*, 933.
- (2) Liu, H. I.; Maluf, N. I.; Pease, R. F. W. *J. Vac. Sci. Technol., B* **1992**, *10*, 2846.
- (3) Namatsu, H.; Horiguchi, S.; Nagase, M.; Kurihara, K. *J. Vac. Sci. Technol., B* **1997**, *15*, 1688.
- (4) Wada, Y.; Kure, T.; Yoshimura, T.; Sudon, Y.; Kobayashi, T.; Goton, Y.; Kondo, S. *J. Vac. Sci. Technol., B* **1994**, *12*, 48.
- (5) Ono, T.; Saitoh, H.; Esashi, M. *Appl. Phys. Lett.* **1997**, *70*, 1852.

- (6) Hasunuma, R.; Komeda, T.; Mukaida, H.; Tokumoto, H. *J. Vac. Sci. Technol., B* **1997**, *15*, 1437.
- (7) Wagner, R. S.; Ellis, W. C. *Appl. Phys. Lett.* **1964**, *4*, 89.
- (8) Givargizov, E. I. *J. Cryst. Growth* **1975**, *32*, 20.
- (9) Boostma, G. A.; Gassen, H. J. *J. Cryst. Growth* **1971**, *10*, 223.
- (10) Westwater, J.; Gosain, D. P.; Tomiya, S.; Usui, S.; Ruda, H. *J. Vac. Sci. Technol., B* **1997**, *15*, 554.
- (11) Lee, S. T.; Wang, N.; Zhang, Y. F.; Tang, Y. H. *Mater. Res. Bull.* **1999**, *24*, 36.
- (12) Morales, A. M.; Lieber, C. M. *Science* **1998**, *279*, 208.
- (13) Zhang, Y. F.; Tang, Y. H.; Wang, N.; Yu, D. P.; Lee, C. S.; Bello, I.; Lee, S. T. *Appl. Phys. Lett.* **1998**, *72*, 1835.
- (14) Yu, D. P.; Lee, C. S.; Bello, I.; Sun, X. S.; Tang, Y. H.; Zhou, G. W.; Bai, Z. G.; Zhang, Z.; Feng, S. Q. *Solid State Commun.* **1998**, *105*, 403.
- (15) Wang, N.; Zhang, Y. F.; Tang, Y. H.; Lee, C. S.; Lee, S. T. *Appl. Phys. Lett.* **1998**, *73*, 3902.
- (16) Wang, N.; Tang, Y. H.; Zhang, Y. F.; Lee, C. S.; Bello, I.; Lee, S. T. *Chem. Phys. Lett.* **1999**, *299*, 237.
- (17) Gole, J. L.; Stout, J. D.; Rauch, W. L.; Wang, Z. L. *Appl. Phys. Lett.* **2000**, *76*, 2346.
- (18) Zhang, Y. F.; Tang, Y. H.; Lam, C.; Wang, N.; Lee, C. S.; Bello, I.; Lee, S. T. *J. Cryst. Growth* **2000**, *212*, 115.
- (19) Zhu, Y. Q.; Hsu, W. K.; Grobert, N.; Terrones, M.; Terrones, H.; Kroto, H. W.; Walton, D. R. M.; Wei, B. Q. *Chem. Phys. Lett.* **2000**, *322*, 312.
- (20) Shi, W. S.; Peng, H. Y.; Zhang, Y. F.; Wang, N.; Shang, N. G.; Pan, Z. W.; Lee, C. S.; Lee, S. T. *Adv. Mater.* **2000**, *12*, 1343.
- (21) Hass, G.; Sulzberg, C. D. *J. Opt. Soc. Am.* **1954**, *44*, 181.